CHAPTER 215

OSCILLATIONS INDUCED BY IRREGULAR WAVES IN HARBOURS

C.R. Chou *, W.Y. Han **

ABSTRACT

An approach for predicting the harbour oscillations induced by undirectional irregular waves in a harbour of arbitrary shape and variable water depth is presented. Effects of partial reflection along harbour and breakwater boundaries were considered by involving an energy dissipation coefficient in boundary conditions.Numerical results on wave heights within a rectangular harbour were presented and a realistic harbour geometry was selected for trial computations. The results of the computations were verified through hydraulic model experiments.

1. INTRODUCTION

One of the major objectives in harbour engineering is the maintenance of a relatively undisturbed water surface within regions of interest. The most effective way to achieve this is to reserve some area in a harbour for natural dissipation. However, almost all the harbours, especially the fishery harbours, in Taiwan have insufficient space to allow for wave energy dissipation. An alternative way is to dispose the vertical dissipating quays in harbours, as many examples are found both in Taiwan and in Japan. However, the choice

---

* Professor,Dept.of Harbour and River Eng.,National Taiwan Ocean Univ., Taiwan, R.O.C.

** Graduate student, ditto.

of the most suitable location and length of the dissipating structure in a harbour is rather problematic. To solve this problem, engineers have usually relied on model experiments in the past, but numerical methods have also been developed. With the increasing speed of performance and lowering cost for acquisition of modern computers, numerical analyses seem to provide a potentially more economical alternative than model experiments.

Many investigators have studied various aspect of the harbour oscillation problem. Miles and Munk(1961) used a point source method to analyze harbour oscillations associated with radiation effects that expand from harbour entrance to offshore. They found the phenomenon of harbour paradox. Ippen and Goda(1963) used Fourier tranformation to analyze a rectangular basin with impermeable veritcal wall. Hwang and Tuck (1970) used a boundary integral method which involves the distribution of wave sources along the harbour boundary to calculate oscillations in harbours of constant depth and arbitrary shape. Lee(1971) applied Weber's solution to solve Helmholtz equation and analyzed harbour oscillation of arbitrary shape with constant water depth. Chou and Lin (1986) used a boundary element method to analyze wave-induced oscillations in a harbour of arbitrary shape, together with rigid quays in variable water depth.

The above studies, however, suffer a deficiency, in other words, they are applicable to complete reflection at the harbour boundaries. In fact, reflecting boundaries are not always fully reflecting. In order to treat this problem, Chou and Lin (1989) applied a boundary element method involving an energy dissipating coefficient $\alpha(=\sqrt{1-Kr^2})$ based on the theory of energy conservation in arbitrary reflecting boundary to analyze oscillations in a harbour of arbitrary shapes with constant water depth. Chou and Han (1993) also applied a boundary element method to analyze oscillations in a harbour of arbitrary shapes with variable water depth.

All of the above studies can be applied only to small amplitude waves. However, waves in seas are one of the most complex and changeable phenomena in nature. In this paper, an extended model for undirectional irregular waves will be presented. For verification, model experiments were carried out and compared with numerical predictions.

2. THEORETICAL ANALYSIS

2.1 Regular Wave

Fig.1 schematically shows a harbour configuration under consideration. A Cartesian coordinate system is employed, the origin of which is located at o with the z-axis vertically upwards. As shown in the figure, the flow field is divided into two regions by a pseudo-boundary surface Γ_1:Region I is an open sea region with constant depth, and Region II is a harbour basin bounded by Γ_1 and the harbour and breakwater boundaries, with variable water depth.

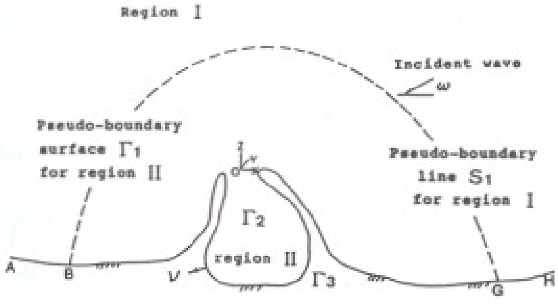

Fig. 1 Definition sketch

Usual assumptions of the fluid being inviscid and incompressible and the flow being irrotational are adopted here. We consider linear waves, having angular frequency $\sigma(= 2\pi/T$, T is the wave period) and amplitude ζ_0 incident from the open sea at an angle of ω against the x-axis. Fluid motions in both the regions will then have velocity potentials as follows:

$$\Phi(x, y, z; t) = \frac{g\zeta_0}{\sigma} \cdot \phi(x, y, z) \cdot \exp(-i\sigma t) \tag{1}$$

where g is the gravitational acceleration, and $\phi(x, y, z)$ must satisfy the Laplace equation $\nabla^2\phi = 0$

Applying Green's law(Chou and Han(1993)), the potential function for any point in Region I can be calculated from the following integral equation:

$$cf^*(x, y) = \int_{s_1} [(\frac{i}{4}H_0{}^{(1)}(kr))\frac{\partial}{\partial\nu}f^*(\xi,\eta) - f^*(\xi,\eta)\frac{\partial}{\partial\nu}(\frac{i}{4}H_0{}^{(1)}(kr))]ds \tag{2}$$

where $f^*(\xi,\eta)$ is the potential function specified by the geometric condition of the boundaries in Region I, $\partial f^*(\xi,\eta)/\partial\nu$ is its normal derivative with ν the local normal coordinate to the boundary taken outwards. $H_0{}^{(1)}(kr)$ is the zeroth order Hankel function of the first kind, and $r = [(x-\xi)^2 + (y-\eta)^2]^{1/2}$ is the distance between a point under consideration and the boundary. The factor c equals to unity within the boundary, but will have a value of 1/2 on boundaries.

In the numerical analysis, the boundary S_1, where c=1/2, is discretized into M segments, each having a constant element. Equation (2) is then rewritten in a matrix form as

$$\{F^*\} = [K^*]\{\overline{F}^*\} \tag{3}$$

where $\{F^*\}$ and $\{\overline{F}^*\}$ are the potential function and its normal derivative on the pseudo-boundary S_1, and $[K^*]$ is a coefficient matrix related to the geometric location of S_1.

According to Green's second identity law, velocity potential $\phi(x, y, z)$ at any point within Region II can be determined as

$$c\phi(x\ ,y\ ,z) = \int \left[\frac{\partial\phi(\xi\ ,\eta\ ,\zeta)}{\partial\nu}(\frac{1}{4\pi r}) - \phi(\xi\ ,\eta\ ,\zeta)\frac{\partial}{\partial\nu}(\frac{1}{4\pi r})\right] dA \tag{4}$$

where $r = [(x-\xi)^2 + (y-\eta)^2 + (z-\zeta)^2]^{1/2}$. As before, c is unity for points inside the region and is equal to 1/2 on smooth boundaries.

To proceed with numerical calculation, surfaces of the boundaries Γ_1 through Γ_4 are divided into N_1 to N_4 discrete segments with constant elements.

For the case that c=1/2, Eq.(4) is readily expressed as

$$\{\phi\} = [K]\{\overline{\phi}\} \tag{5}$$

where $\{\phi\}$ and $\{\overline{\phi}\}$ are the potential function and its normal derivative on the boundaries Γ_1 through Γ_4. [K] is a coefficient matrix related to the geometry of the boundaries.

The boundary conditions required for the case under consideration are summarized as follows:

(i) The free surface condition:

For constant air pressure, the kinematic boundary condition for the free water surface is expressed as:

$$\overline{\phi} = \frac{\sigma^2}{g} \cdot \phi \quad , \quad z = 0 \tag{6}$$

(ii) Boundary condition on impermeable sea bed:

For an impermeable sea floor, the flow is zero in the normal direction:

$$\overline{\phi} = 0 \tag{7}$$

(iii) Boundary condition on the pseudo-boundary at open sea:

The requirement of continuity for mass and energy fluxes between Region I and Region II at the pseudo-boundary Γ_1 leads to the expression:

$$\overline{\phi}_0(\xi, \eta, z) = \overline{\phi}(\xi, \eta, z) \tag{8}$$

$$\phi_0(\xi, \eta, z) = \phi(\xi, \eta, z) \tag{9}$$

(iv) Boundary condition on a quay or breakwater

Assume the boundaries of the quays or breakwaters Γ_3 are impermeable and have an arbitrary coefficient of reflection K_r. Since waves are reflected only partially, based on the theory of energy conservation,these constructions can therefore be treated, conceptually, as having a energy dissipating coefficient α indicated by Chou and Lin(1989) reads

$$\alpha = \sqrt{1 - {K_r}^2} \tag{10}$$

The boundary condition on Γ_3 can be expressed conveniently as:

$$\overline{\phi}(\xi, \eta, \zeta) = ik\alpha\phi(\xi, \eta, \zeta) \tag{11}$$

Substitution of Eqs.(6),(8),(9) and (11) into Eq.(5), a little algebra lead to

$$\begin{bmatrix} [K_{11} - CRK^*Q] & \frac{\sigma^2}{g} K_{12} & ik\alpha K_{13} \\ K_{21} & \frac{\sigma^2}{g} K_{22} - I & ik\alpha K_{23} \\ K_{31} & \frac{\sigma^2}{g} K_{32} & ik\alpha K_{33} - I \end{bmatrix} \begin{bmatrix} \overline{\phi}_1 \\ \phi_2 \\ \phi_3 \end{bmatrix} = \begin{bmatrix} R[F^o - K^* \overline{F}^o] \\ 0 \\ 0 \end{bmatrix} \tag{12}$$

where $C = k/(N_0 \sinh kh)$, $\{F^o\}$ and $\{\overline{F}^o\}$ are the potential function and its normal derivative of the incident wave, [R] and [Q] are coefficient matrices given by Chou and Han (1993).

By solving the above equation, the potential functions on boundaries Γ_2 are obtained. The wave height ratio, K_d, defined as the ratio of the wave height in Region II to the incident wave height, can be calculated from

$$K_d = |\phi_2| \tag{13}$$

2.2 Irregular Wave

The approach for the oscillations of undirectional irregular waves in the harbour of arbitrary shape with dissipating quays is based on the spectral resolution method (Nagai (1972)), where each component wave is known. Assuming that incident component waves are small amplitude waves, the oscillations of these regular waves can be obtained by numerical method in section 2.1 ,then the water surface oscillations for irregular waves can be obtained through linear superposition method.

In this paper, the Bretschneider spectrum (Bretschneider(1968)) was used. In order to simplify the process of numerical analysis, the incident spectrum was transformed into dimensionless type as follows:

$$S^*(f^*) = af^{*-5}\exp[-(bf^{*-4})] \tag{14}$$
$$a = b/4$$
$$b = 0.675/0.9^4 = 1.0288$$

To obtain the component waves, the dimensionless spectrum is discretized into m parts, each with the same energy ΔE (each part under the spectrum having the same area), then, the representive frequencies $f_{cn}{}^*$ of each component wave can be written as

$$f_{cn}{}^* = \sqrt{\frac{8am\sqrt{\pi}}{\sqrt{b}}\left[erf\left(\sqrt{2\ln\left(\frac{m}{n-1}\right)}\right) - erf\left(\sqrt{2\ln\left(\frac{m}{n}\right)}\right)\right]} \tag{15}$$

where a and b are the coefficients of the dimensionless Bretschneider spectrum; n=1,2,....m; and $erf(x)$ is the error function given as

$$erf(x) = \int_0^x \frac{\exp(-z^2/2)}{\sqrt{2\pi}}dz \tag{16}$$

2.3 Wave height ratio K_D and period ratio K_T due to irregular waves

From section 2.1, the wave height ratio K_d due to regular component waves can be obtained, then the wave height ratio K_D and period ratio K_T due to irregular waves can be obtained by following equations.

$$K_D = \frac{H_{1/3}}{(H_{1/3})_o} = 4.0\sqrt{\int_0^\infty S_D^*(f^*)df^*} \tag{17}$$

$$K_T = \frac{T_{1/3}}{(T_{1/3})_o} = \sqrt[4]{\pi b}\sqrt{\frac{\int_0^\infty S_D^*(f^*)df^*}{\int_0^\infty f^{*2} S_D^*(f^*)df^*}} \tag{18}$$

$$S_D^*(f^*) = K_d^2 S^*(f^*) \tag{19}$$

where $S_D^*(f^*)$ is the spectrum in the harbour induced by the incident spectrum $S^*(f^*)$, subscript "o" means the values in off-shore.

3. DETERMINATION OF THE REFLECTION COEFFICIENT

To proceed with the analysis numerically, the energy dissipation coefficient α in Eq.(11) must be determined. In other words,the reflection coefficient of the dissipating structure in Eq.(10) must be found empirically. This was done in a 2-D wave flume, shown schematically in Fig.2. The reflection coefficients can be obtained as shown in Fig.3, where the dotted curve shows the best fit of the experimental data in a least squares sense. Reflection coefficients for different frequencies determined from this empirical function were used in the subsequent calculations.

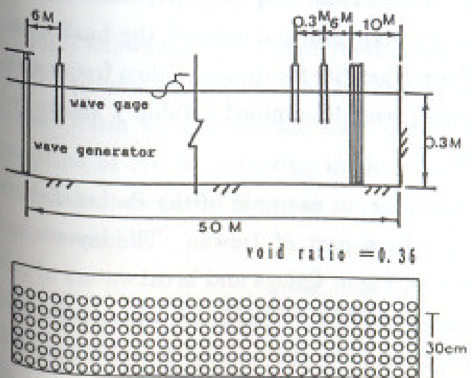

Fig. 2 Setup of 2-D wave flume & dissipating quay

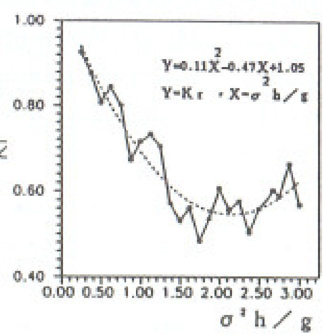

Fig. 3 The reflection coefficient of dissipating quay

4. EXAMPLE

Table 1. Cases of square basin

	S1	S2	S3	remarks
case I	×	×	×	× : impermeable quay
case II	○	○	○	○ : dissipating quay
case III	×	○	×	
case IV	○	×	○	

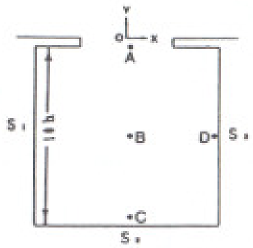

Fig. 4 Definition sketch for square harbour

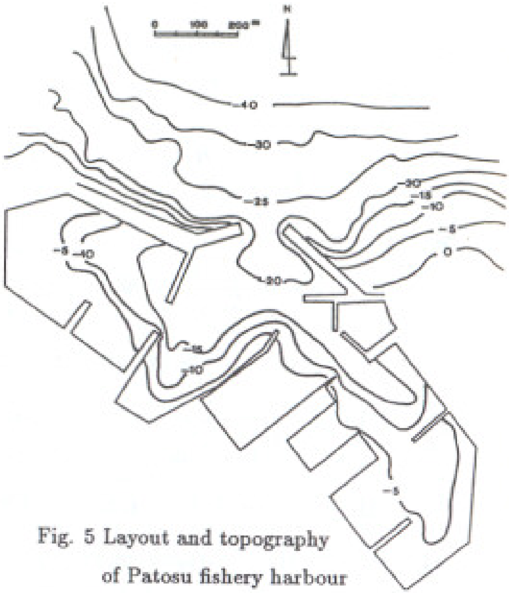

Fig. 5 Layout and topography of Patosu fishery harbour

Calculations were first carried out for a square basin with a width equal to 10h,(h is the water depth of the open sea) and an opening width b=5h at the center of the basin, as shown in Fig.4. The same dissipating quays as those in the two-dimensional wave flume experiment were assumed and uniform water depths in both the Regions I and II.

In the numerical analysis, the surfaces of the boundaries are divided into 1056 discrete areas with constant element (N_1=104 ,N_2=720 ,N_3=52 , N_4=180,M=2). Waves propagating perpendicular toward the harbor entrance were used. Distributions of wave heights for dimensionless frequencies $\sigma^2_{1/3}h/g = 1.206$ ($T_{1/3} = 1.0$ second) was determined. Table 1 shows the conditions used for the calculation.

Computations were also performed for an example of the Patosu fishery harbour built 3 years ago in the northern part of Taiwan. The layout and topography of the harbour are given in Fig.5. Quays and breakwaters of this fishery harbour are dissipating structures (PERFORCELL), whose reflection coefficient is estimated approximately at 0.75, the energy dissipation coefficient being 0.661. In the numerical computation, water depth larger than 40 m was regarded as constant, and the boundary surfaces were divided into 1988 discrete segments with constant elements (N_1=152,N_2=1329,N_3=176,N_4=331 and M=2). Distributions of wave heights were calculated for incident waves propagating from 23.5° north-northeast ($\omega = 66.5°$) toward the harbour entrance with dimensionless frequencies of $\sigma_{1/3}^2 h/g = 1.611$ ($T_{1/3} = 1.0$ second).

In the numerical analysis, the dimensionless spectrum is discretized into 12 segments(m=12), then the representive frequency f_{cn}^* of each component wave can be calculated by Eq.15, and the wave height ratio K_D and period ratio K_T can be obtained by Eq.17 to 18.

5. LABORATORY EXPERIMENT

Experiments were carried out in a 3-D wave basin. The wave basin is 30 m long, 24 m wide and 1 m deep. The programmable wave generator is capable of generating regular and irregular waves. Water depth was kept to be 0.3m throughout the experiments. Water surface displacements were measured with capacitance-type wave gauges.

6. RESULTS AND DISCUSSION

Fig.6 shows the wave height distributions for irregular waves obtained both by the present numerical method and experiments for case I and case II of square basin with significant wave period $(T_{1/3})_0$ =1.0 second. From these figures, a general increase of wave height in case I due to reflection effects and decrease of that in case II due to the effects of disposing dissipating quays were found. The tendencies of wave height distributions predicted by the present numerical model are confirned by the experiments.

Fig.7 shows the period distributions K_T for irregular waves obtained both by the present numerical method and experiments for case I and case II of square basin with significant wave period $(T_{1/3})_0$ =1.0 second. The spatial variation of K_T is increasing in the range of 20% in the square basin, and the spatial similarity between numerical solutions and experimental results are reasonable.

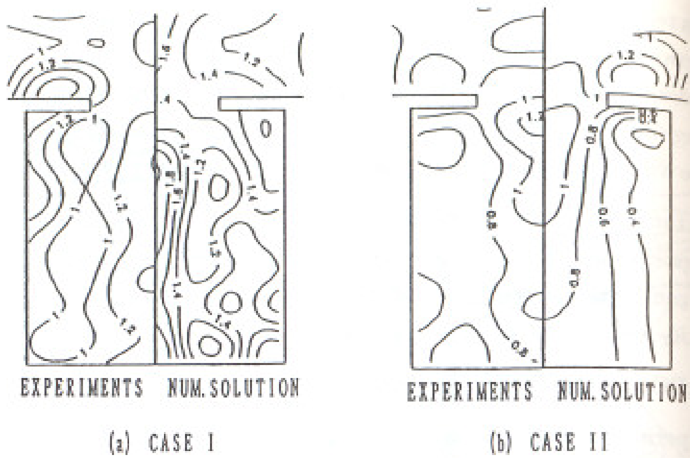

Fig.6 Wave height distributions K_D for irregular wave $(\sigma_{1/3})^2 h/g$=1.206, t=1.0 sec, h=30 cm, $\omega = 90^o$

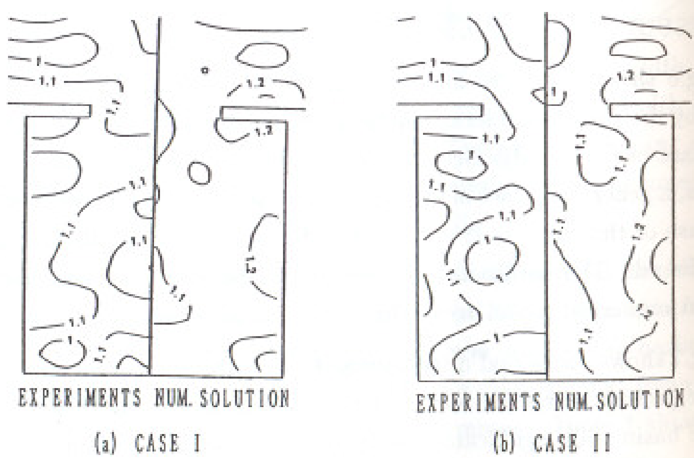

Fig.7 Wave height distributions K_T for irregular wave $(\sigma_{1/3})^2 h/g$=1.206, t=1.0 sec, h=30 cm, $\omega = 90^o$

Fig.8 shows the comparision of wave height distributions in square basin by numerical model to regular waves with period T=1.0 second and to irregular waves with significant period $(T_{1/3})_0$ =1.0 second for case I to IV respectively. For both regular and irregular waves, the oscillations in case II to IV is apparently reduced because of disposing dissipating quays. Compared the difference of wave height distributions induced by regular and irregular waves, it can be found that the wave height distributions induced by irregular waves are, in general, more stable than those induced by regular waves. The wave motions by irregular waves generally consist with those existing in nature sea-water surface.

Fig.9 shows the distribution of wave height K_D for irregular wave obtained by the numerical method and experiments for the Patosu fishery harbour with $\alpha = 0.661$, wave direction of 23.5° north-northeast and wave period $(T_{1/3})_0$ =1.0 second. Compared the difference of these figures with Fig.10 , the same phonemona in square basin metioned above that the wave height distributions induced by irregular waves are more stable than those induced by regular waves was found. The spatial similarity between numerical solutions and experimental results are reasonable too.

Fig.10 shows the period distributions K_T for irregular waves obtained both by the present numerical method and experiments for the Patosu fishery harbour with significant wave period $(T_{1/3})_0$ =1.0 second. The spatial variation of K_T is increasing in the range of 20% in the numerical results. Because the wave heights in the inner region of the harbour are too small to measured, the significant wave period in that region can not be obtained in the laboratory.

7.CONCLUSION

The effects of dissipative quays and/or breakwaters are modeled using a coefficient for energy dissipation in the boundary condition. Comparisons of calculated and measured resluts for both a square basin and a real harbour are shown. From the examples presented above show that the spatial similarity between numerical solutions and experimental results are reasonable. it is conjectured that, given the correct coefficient, the most suitable position for disspating quays in a harbour could be estimated by the present method.

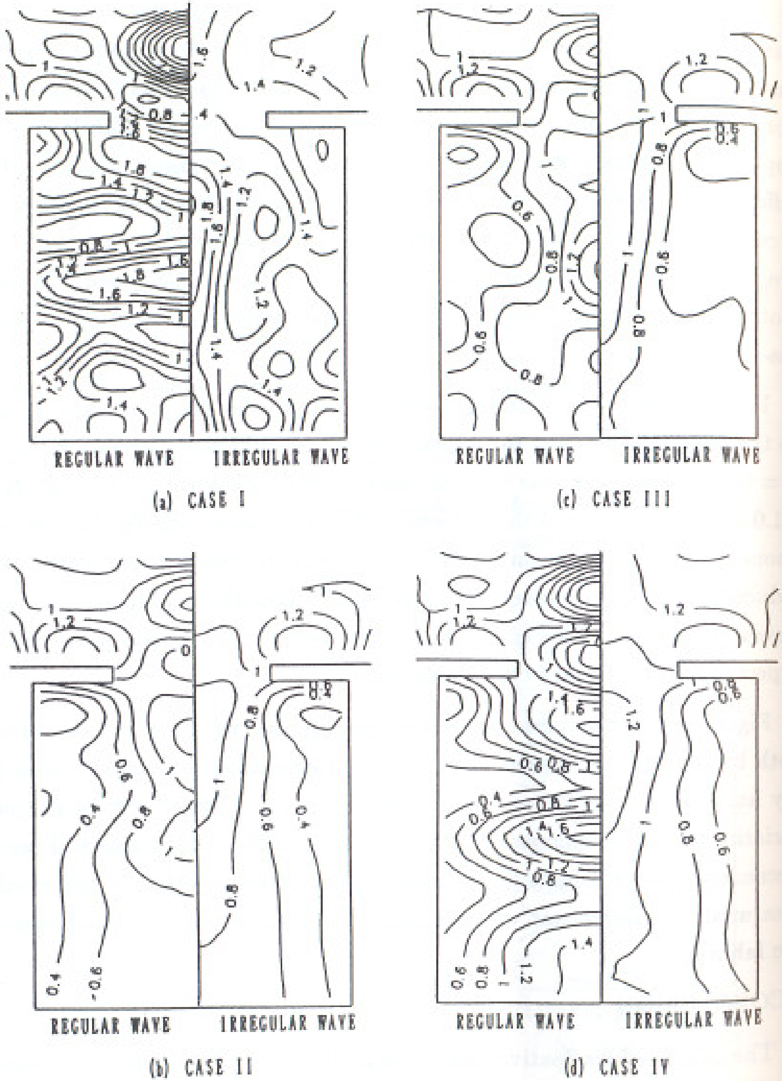

Fig.8 Wave height distributions for regular wave (T=1.0 sec.)

and irregular wave ($T_{1/3}$=1.0 sec.)

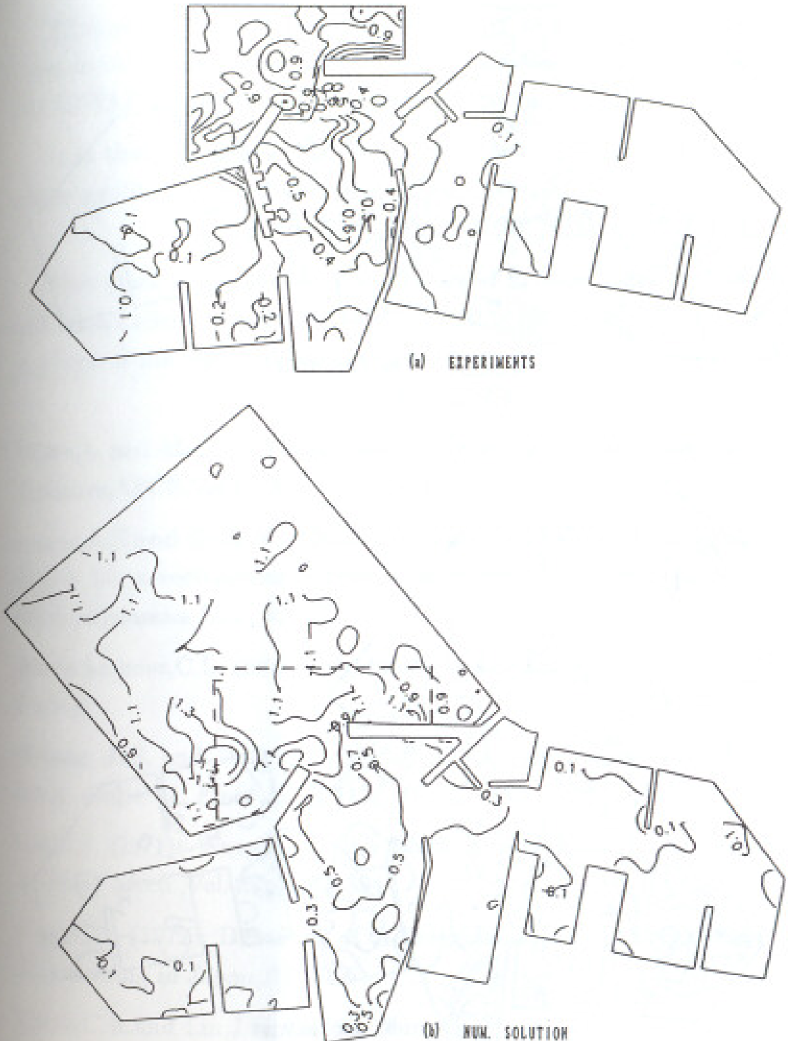

Fig.9 Wave height distributions K_D for irregular wave in Patosu fishery harbour,($T_{1/3}$=1.0 sec.)

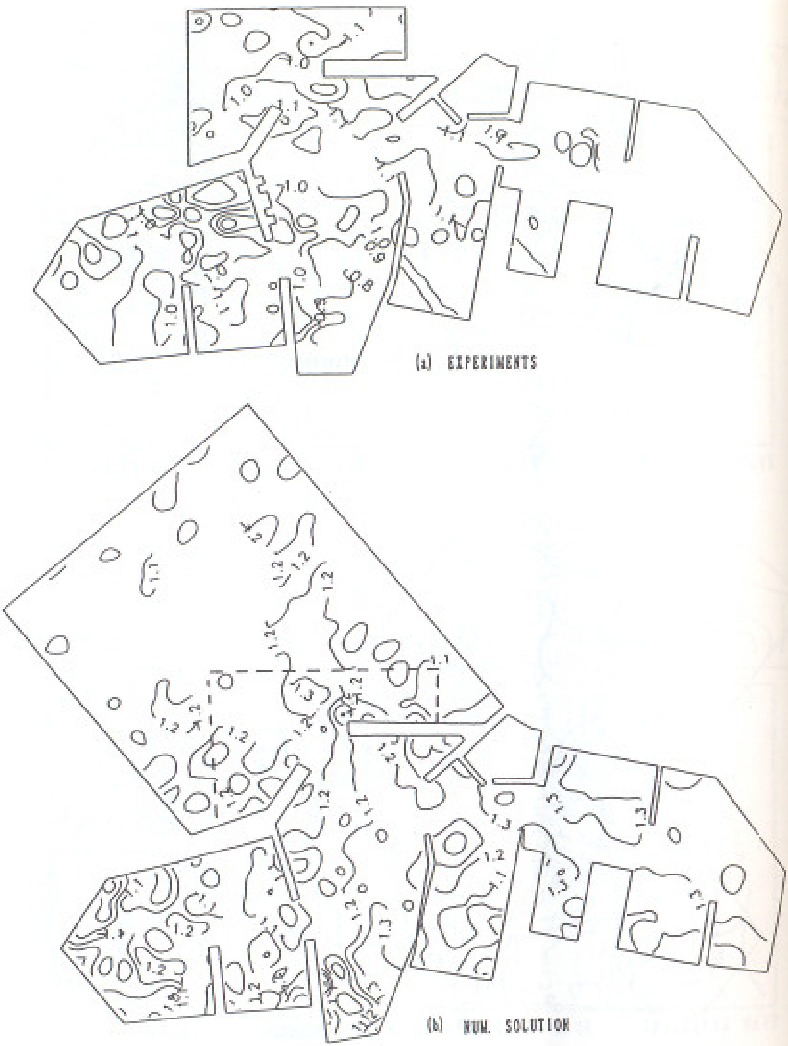

Fig.10 Wave period distributions K_T for irregular wave in Patosu fishery harbour,($T_{1/3}$=1.0 sec.)

Though only the Bretschneider spectrum as incident wave spectrum was used in this paper, other spectrums such as Pierson Moskowitz spectrum or JONSWAP spectrum can be applied by this method also.

It is thus concluded that the present numerical method can be used to study problems related with harbour oscillations.

ACKNOWLEDGEMENTS

This work is sponsored by the National Science Council of the Republic of China under the grant No. NSC 81-0209-E-019-3, the advice and financial support of the National Science Council are gratefully acknowledged.

REFERENCE

Miles,J. and Munk,W.(1961): Harbors paradox; *J. Waterways and Harbors Division*,ASCE,Vol.87,No.WW3,pp111-130.

Ippen,A.T.and Goda,Y. (1963): Wave-induced oscillations in harbors:the solution for a rectangular harbor connected to the open-sea; *Report.No.59, Hydrodynamics Lab.*, M.I.T.

Bretschneider,C.L. (l968): Significant waves and wave spectrum, Ocean Industry.

Hwang ,L.S. and Tuck ,E.O. (1970): On the oscillations of harbors of arbitrary shape. ,*J. Fluid Mech.* ,42.

Lee,J.J. (l971): Wave-induced oscillations in harbors of arbitrary geometry; *J. Fluid Mech.*,Vol.45,pp.375-394.

Nagai,K., (1972): Difraction of the irregular sea due to breakwaters, *Coastal Engineering in Japan*,JSCE.15

Chou,C.R.and Lin,J.G. (1986): Numerical analysis for harbor oscillation of arbitrary shape in uneven sea bed by BEM;*8th Conf. on Ocean Engng.*, R.O.C., pp.111-130.(in Chinese)

Chou,C.R.and Lin,J.G. (1989): Numerical analysis for harbor oscillation with wave absorber;*11th Conf. on Ocean Engng.*, R.O.C., pp.365-381.(in Chinese)

Chou,C.R.and Han,W.Y.(1993): Wave-induced oscillations in harbours with dissipating quays; *Journal of Coastal Engineering in Japan*, Vol. 36, No.1, pp.1-23.